Theory of Rare B Decays: $b \to s\gamma$ and $b \to s\ell^+\ell^-$

Thomas Mannel

Institut für Theoretische Teilchenphysik, Universität Karlsruhe, 76128 Karlsruhe, Germany

Abstract. In this lectures some of the theoretical aspects of rare B decays are discussed. The focus is on inclusive decays, since these can be computed more reliably. Topics covered are (1) short distance effects, (2) long distance QCD effects and (3) effects of "new physics" in these decays.

1 Introduction: $\mathcal{H}_{eff}$ for $b \to s\gamma$ and $b \to s\ell^+\ell^-$

These lectures are devoted to a discussion of rare B decays, focussing on so called flavour changing neutral current (FCNC) decays of the type $b \to s\gamma$ and $b \to s\ell^+\ell^-$. In the standard model these processes cannot appear at tree level and hence are loop-induced transitons. Thus they constitute an important check of the standard model and may open a window on physics beyond this model.

Radiative rare B decays have attracted considerable attention in the last few years. After the first observation in 1994, by the CLEO collaboration [1], data have become quite precise [2] so that even a measurement of the CP asymmetry in these decays [3] became possible. As far as data are concerned, the situation clearly will improve further, after the excellent start of both B factories at KEK and at SLAC.

$B \to X_s\gamma$ as well as $B \to X_s\ell^+\ell^-$ test the Standard Model (SM) in a particular way. The GIM cancellation, which is present in all the FCNC processes, is lifted in this case by the large top-quark mass; if the top quark were as light as the b quark, these decays would be too rare to be observable.

Since the SM contribution is small, these decays have a good sensitivity to "new physics", e.g. to new (heavy) particles contributing to the loop. In fact, already the first CLEO data could constrain some models for "new physics" in a stringent way[1].

The most general effective Hamiltonian describing the decays of the type $b \to s\gamma$ is given by

$$H_{eff} = \sum_i c_i \, O_i \,, \tag{1}$$

where the O_i are local operators

$$\begin{aligned} O_{1\cdots 6} &= \text{four-fermion operators} \\ O_7 &= m_b \bar{s}\sigma_{\mu\nu}(1+\gamma_5) b \, F^{\mu\nu} \\ O_7' &= m_s \bar{s}\sigma_{\mu\nu}(1-\gamma_5) b \, F^{\mu\nu} \end{aligned}$$

T. Mannel, Theory of Rare B Decays: $b \to s\gamma$ and $b \to s\ell^+\ell^-$, Lect. Notes Phys. **647**, 78–99 (2004)
http://www.springerlink.com/

$$\begin{aligned} O_8 &= m_b \bar{s}\sigma^{\mu\nu}T^a(1+\gamma_5)b\,G^a_{\mu\nu} \\ O'_8 &= m_s \bar{s}\sigma^{\mu\nu}T^a(1-\gamma_5)b\,G^a_{\mu\nu} \end{aligned} \tag{2}$$

and c_i are pertubatively calculable coefficients.

In any new physics analysis of B decays only the coefficients c_i are tested [4]. The decay $B \to X_s\gamma$ (and the corresponding exclusive decays) are practically determined by the two operators O_7 and O'_7, and hence these decays are mainly testing c_7 and c'_7. In the SM these two coefficients are

$$c_7 = -\frac{G_F^2 e}{32\sqrt{2}\pi^2} V_{tb}V_{ts}^* C_7 m_b, \tag{3}$$

$$c'_7 = -\frac{G_F^2 e}{32\sqrt{2}\pi^2} V_{tb}V_{ts}^* C_7 m_s \tag{4}$$

where C_7 is a function of $(m_t/M_W)^2$, which we shall discuss later.

Furthermore, the two operators differ by the handedness of the quarks; in order to disentangle these two contributions there has to be a handle on the polarization of the quarks or of the photon, which is impossile at a B factory. Consequently, from $b \to s\gamma$ alone only the combination $|c_7|^2 + |c'_7|^2$ can be determined in the near future.

Once the effective interaction for the quark transition is fixed, one has to calculate from this the actual hadronic process. This step is only for the inclusive decays under reasonable theoretical control; for exclusive decays, form factors are needed, which either need to be modelled or will finally come from the lattice.

For inclusive decays the machinery used is the heavy mass expansion[1]. Using this framework for the total rate one can establish that (1) the leading term as $m_b \to \infty$ is the free quark decay, (2) there are no subleading corrections of order $1/m_b$, (2) the first non-vanising corrections are of order $1/m_b^2$ and are given in terms of two parameters. This will be discussed in Sect. 3. Additional non-perturbative uncertainties are induced by a cut on the photon energy, which is necessary from the exprimental point of view to suppress backgrounds.

One may discuss the decays $b \to s\ell^+\ell^-$ in a similar way. Here we have to extend the operator basis (2) by two more operators involving leptons

$$\mathcal{O}_9 = \frac{\alpha}{\alpha_s}(\bar{s}_{L\alpha}\gamma_\mu b_{L\alpha})(\bar{\ell}\gamma^\mu \ell) \tag{5}$$

$$\mathcal{O}_{10} = (\bar{s}_{L\alpha}\gamma_\mu b_{L\alpha})(\bar{\ell}\gamma^\mu\gamma_5 \ell) \tag{6}$$

This involves two more wilson coefficients C_9 and C_{10} and the contribution of these two operators have tp be added to the effective Hamiltonian (1).

The QCD corrections to the effective hamiltonian (1) have been calculated already to next-to-leading order. A detailed review on this subject is given in [10]. The value of the coefficients at subldeading order involves subtelties such as the question of how to deal with γ_5 in dimensional regularization. We do

[1] A non-exhaustive selection of revies is [5–9].

not want to discuss these points in this lecture, although some of the results for $B \to X_s\gamma$ are quoted at NLLO precision. In order to give some feeling for the size of the Wilson coefficients we quote in Table 1 their values at leading logarithmic acuracy, where the abovementioned subtelties do not matter.

Table 1. Values for the Wilson coefficients $C_i(\mu)$ at the scale $\mu = m_W$ ("matching conditions") and at three other scales, $\mu = 10.0$ GeV, $\mu = 5.0$ GeV and $\mu = 2.5$ GeV, evaluated with one-loop β-function and the leading-order anomalous-dimension matrix, with $m_t = 174$ GeV and $\Lambda_{\rm QCD} = 225$ MeV. Note that the relation between c_i appearing in (1) and the tabulated coefficients is $c_i = 4G_F V_{ts}^* V_{tb} C_i/\sqrt{2}$; furthermore, $C_9'(\mu) \equiv C_9(\mu)/\alpha_s(\mu)$ (see secction 6.1).

$C_i(\mu)$	$\mu = m_W$	$\mu = 10.0$	$\mu = 5.0$	$\mu = 2.5$
C_1	0.0	0.182	0.275	0.40
C_2	-1.0	-1.074	-1.121	-1.193
C_3	0.0	-0.008	-0.013	-0.019
C_4	0.0	0.019	0.028	0.040
C_5	0.0	-0.006	-0.008	-0.011
C_6	0.0	0.022	0.035	0.055
C_7	0.195	0.286	0.325	0.371
C_8	0.097	0.138	0.153	0.172
C_9'	-2.08	-2.31	-2.36	-2.38
C_{10}	4.54	4.54	4.54	4.54

2 Perturbative Corrections to $b \to s\gamma$

The main perturbative corrections are the QCD corrections, which are substantial. These corrections are calculated using an effective field-theory framework and yield the QCD corrections to the Wilson coefficents.

To set this up, we have to write down first the relevant effective Hamiltonian as in (1). The operators appearing in (1) mix under renormalization as we evolve down from the M_W mass scale to the relevant scale, which is the mass of the b quark. The cofficient functions are calculated at the scale $\mu = M_W$ as a power series in the strong coupling

$$c_i(M_W) = c_i^{(0)}(M_W) + \frac{\alpha_s(M_W)}{\pi} c_i^{(1)}(M_W) + \cdots \tag{7}$$

Changing the scale μ results in a change of the coefficient functions and in the matrix elements, such that the matrix element of the effective Hamiltonian remains μ-independent. This change can be computed perturbatively for sufficiently large μ, using the standard machinery of renormalization group, which involves a calculation of the anomalous-dimension matrix that describes the mixing of the operators (2).

The solution of the renormalizaton group equation yields the coefficient functions at some lower scale μ, which take the form (schematically)

$$c_i(\mu) = c_i^{(0)}(M_W) \sum_{n=0} b_n^{(0)} \left(\frac{\alpha_s}{\pi} \ln \left(\frac{M_W^2}{\mu^2} \right) \right)^n + \frac{\alpha_s}{\pi} c_i^{(1)}(M_W) \sum_{n=0} b_n^{(1)} \left(\frac{\alpha_s}{\pi} \ln \left(\frac{M_W^2}{\mu^2} \right) \right)^n + \cdots \tag{8}$$

where the b_n are obtained from the solution of the renormalization group equation.

The last step is to compute the matrix elements of the operators at a scale $\mu \approx m_b$. This can be done for the inclusive case using the $1/m_b$ expansion. For the exclusive case, one would need the form factor in the corresponding approximation, which cannot be done with present theoretical techniques.

At present, the leading and the subleading terms of the coefficients have been calculated [11–14], including electroweak contributions[15], the main part of which is due to the correct scale setting in α_{em}.

A complete and up-to-date compilation can be found in [16]. Without going into any more detail we only quote the result from [16]

$$Br(B \to X_s\gamma) = (3.29 \pm 0.33) \times 10^{-4}\,. \tag{9}$$

where this result includes a cut on the photon energy at $E_{\gamma,min} = 0.05\, m_b$.

The QCD corrections are in fact dramatic; they increase the rate for $b \to s\gamma$ by about a factor of two. For example, already at the leading-log level we have $c_7(m_b)/c_7(M_W) = 1.63$, see Table 1. Another indication of this fact is a substantial dependence of the leading-order result on the choice of the renormalization scale μ. This is usually estimated by varying the scale μ between $m_b/2$ and $2m_b$. In this way one obtains a variation of $\delta_\mu = {}^{+27.4\%}_{-20.4\%}$ for the leading-order result.

Taking into account the subleading terms reduces the scale dependence substantially. In fact, one has at subleading order [16] $\delta_\mu = {}^{+0.1\%}_{-3.2\%}$, which is smaller than naively expected [17]. It has been argued that the smallness of δ_μ is accidental [16]. However, arguments have been given recently [18] that these cancellations are not accidental. In fact, most of the large radiative corrections may be assigned to the running of the b quark mass appearing in the operator O_7.

3 Non-perturbative Corrections to $b \to s\gamma$

Non-perturbative corrections arise from different sources. We shall consider here

- Long-distance effects from intermediate vector mesons $B \to J/\Psi X_s \to X_s\gamma$,
- Subleading terms in the heavy mass expansion: $1/m_b$ and $1/m_c$ corrections,
- Non-perturbative contributions to the photon spectrum ("shape function").

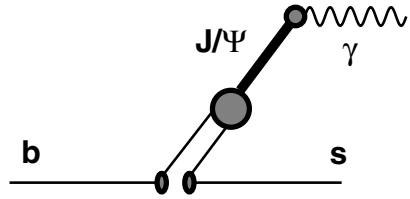

Fig. 1. Long distance contribution $B \to J/\Psi X_s \to X_s\gamma$

3.1 $B \to J/\Psi X_s \to X_s\gamma$

One long-distance contribution comes from the process $B \to X_s J/\Psi$ and the subsequent decay of the (off-shell) J/Ψ into a photon, see Fig. 1. The first process $B \to X_s J/\Psi$ has a branching ratio of order 1%, at least for an on-shell J/Ψ. Assuming that this is similar for the off-shell case, we have to multiply it with another factor $1/m_c^2$ for the propagation of the J/Ψ and a factor $f_{J/\Psi}^2$, since the J/Ψ has to annihilate into a photon. This leads us to the conclusion that this contribution is indeed negligibly small. However, one has to keep in mind that some extrapolation from $q^2 = m_{J/\Psi}^2$ to $q^2 = 0$ is involved, assuming that this will not lead to a strong enhancement.

3.2 $1/m_b$ and $1/m_c$ Corrections

A set of "standard" non-perturbative corrections arises from the heavy mass expansion [5–9]. As far as the total rate is concerned, we have the subleading corrections of order $1/m_b^2$, which are parametrized in terms of the kinetic energy λ_1 and the chromomagnetic moment λ_2 defined by the matrix elements

$$2M_H\lambda_1 = \langle H(v)|\bar{h}_v(iD)^2 h_v|H(v)\rangle \tag{10}$$

$$6M_H\lambda_2 = \langle H(v)|\bar{h}_v\sigma_{\mu\nu}iD^\mu iD^\nu h_v|H(v)\rangle\,. \tag{11}$$

In terms of these two matrix elements the total rate reads at tree level up to order $1/m_b^2$

$$\Gamma = \frac{G_F^2\alpha m_b^5}{32\pi^4}|V_{ts}V_{tb^*}|^2|C_7|^2\left(1 + \frac{\lambda_1 - 9\lambda_2}{2m_b^2} + \cdots\right). \tag{12}$$

This result is fully integrated over the photon energy spectrum. One can also compute the energy spectrum of the photon within the $1/m_b$ expansion, which is given, again at tree level, by

$$\frac{d\Gamma}{dx} = \frac{G_F^2\alpha m_b^5}{32\pi^4}|V_{ts}V_{tb^*}|^2|C_7|^2 \tag{13}$$
$$\left(\delta(1-x) - \frac{\lambda_1 + 3\lambda_2}{2m_b^2}\delta'(1-x) + \frac{\lambda_1}{6m_b^2}\delta''(1-x) + \cdots\right)$$

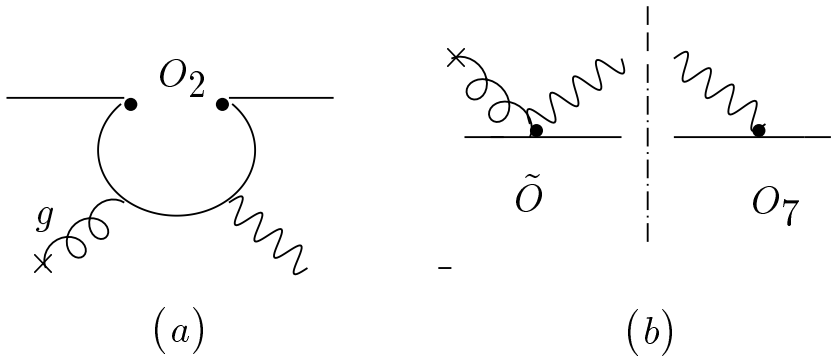

Fig. 2. Interference between O_7 and one of the four-fermion operators (O_2), leading to a contribution of order $1/m_c^2$

which can only be interpreted in terms of moments of the spectrum. We shall return to this point in the next subsection.

If the charm quark is also assumed to be heavy, one may discuss the charm-mass dependence in terms of a $1/m_c$ expansion [19]. The relevant contribution originates from the four-fermion operators (e.g. the operator O_2) involving the charm quark, see Fig. 2. Expanding the matrix element of O_2 in powers of $1/m_c$ we obtain a local operator of the form

$$O_{1/m_c^2} = \frac{1}{m_c^2}\bar{s}\gamma_\mu(1-\gamma_5)T^a b\, G^a_{\nu\lambda}\epsilon^{\mu\nu\rho\sigma}\partial^\lambda F_{\rho\sigma} \tag{14}$$

which can interfere with the leading term O_7 (see Fig. 2).

The detailed calculation [20,21] reveals that this contribution is rather small

$$\frac{\delta\Gamma_{1/m_c^2}}{\Gamma} = -\frac{C_2}{9C_7}\frac{\lambda_2}{m_c^2} \approx 0.03 \tag{15}$$

3.3 Non-perturbative Corrections in the Photon Energy Spectrum

The non-perturbative corrections for the total rate are thus quite small and can safely be neglected against the perturbative ones. However, to extract the process $B \to X_s\gamma$ there has to be a lower cut on the photon energy to get rid of the uninteresting processes such as ordinary bremsstrahlung. Clearly it is desirable to have this cut as high as possible, but this makes the process "less inclusive" and hence more sensitive to non-perturbative contributions to the photon-energy spectrum.

Since we are dealing at tree level with a two-body decay, the naive calculation of the photon spectrum yields a δ function at partonic level and the $1/m_b^n$ corrections are again distributions located at the partonic energy $E_\gamma = m_b/2$, see (13). Clearly (13) cannot be used to implement a cut on the photon energy spectrum, since this is not a smooth function.

The perturbative contributions have been calculated and yield a spectrum that is mainly determined by the bremsstrahlung of a radiated gluon. This part of the calculation is fully perturbative and enters the next-to-leading order analysis described in the previous section. In particular, the partonic δ function smoothens and turns into "plus distributions" of the form

$$\frac{d\Gamma}{dx} = \cdots + \frac{\alpha_s}{\pi}\left[\left(\frac{\ln(1-x)}{1-x}\right)_+ , \left(\frac{1}{1-x}\right)_+\right] , \tag{16}$$

where the ellipses denote terms that are regular as $x \to 1$ and contributions proportional to $\delta(1-x)$, which are determined by virtual gluons.

Here we shall focus on the non-perturbative contributions close to the endpoint. The general structure of the terms in the $1/m_b$ expansion is

$$\frac{d\Gamma}{dx} = \Gamma_0\left[\sum_i a_i \left(\frac{1}{m_b}\right)^i \delta^{(i)}(1-x) + \mathcal{O}((1/m_b)^{i+1}\delta^{(i)}(1-x))\right] , \tag{17}$$

where $\delta^{(i)}$ is the ith derivative of the δ function.

It has been shown [22,23] that the terms with $\delta^{(i)}(1-x)/m_b^i$ can be resummed into a non-perturbative function such that the photon energy spectrum becomes

$$\frac{d\Gamma}{dx} = \frac{G_F^2 \alpha m_b^5}{32\pi^4}|V_{ts}V_{tb^*}|^2|C_7|^2 f(m_b[1-x]) , \tag{18}$$

where the non-perturbative fuction f is formally defined by the matrix element

$$2M_B f(\omega) = \langle B|\bar{Q}_v \delta(\omega + iD_+)Q_v|B\rangle . \tag{19}$$

Here D_+ is the light-cone component of the covariant derivative, acting on Q_v, which denotes a heavy-quark field in the static approximation.

The shape function is in fact a universal function, which appears for any heavy-to-light transition in the corresponding kinematical region. In general these transitions should be written as a convolution of a (perturbatively calculable) Wilson coefficient and the non-perturbative matrix element

$$d\Gamma = \int d\omega\, C_0(\omega)\langle B|O_0(\omega)|B\rangle \tag{20}$$

with

$$O_0(\omega) = \bar{Q}_v \delta(\omega + iD_+)Q_v \tag{21}$$

At tree level this leads to a simple and intuitive formula in which the mass m_b is replaced by an "effective mass" $m_b^* = m_b - \omega$ such that

$$d\Gamma = \int d\omega\, d\Gamma_{tree}(m_b \to m_b^*) f(\omega) \tag{22}$$

Since this function is universal, it appears in the semileptonic $b \to u\ell\bar{\nu}$ transitions as well as in the $b \to s\gamma$ decays. At leading twist, this leads to a model-independent relation between these inclusive decays, which may be used to obtain $|V_{ts}/V_{ub}|$ [25,24].

Moments of the shape function can be related to the parameters describing the subleading effects in the $1/m_b$ expansion. One has

$$\int d\omega\, f(\omega) = 1\,, \quad \int d\omega\, \omega\, f(\omega) = 0\,, \tag{23}$$
$$\int d\omega\, \omega^2\, f(\omega) = -\frac{\lambda_1}{3m_b^2}\,, \quad \int d\omega\, \omega^2\, f(\omega) = -\frac{\rho_1}{3m_b^2}\,.$$

Radiative corrections can be included using the machinery of effective field theory. However, here some ambiguity arises from the appearance of a double logarithm (see (16)), which makes the matching ambiguous. Various authors [25,26] have used the mass convolution formula (22), although this has not yet been proven to be correct beyond the tree level.

Finally one may also try to resum the subleading terms in $1/m_b$, i.e. the terms of order $\delta^{(i)}(1-x)/m_b^{i+1}$ in (17). This has been discussed in [27], where it has been shown that the relevant operators are

$$O_1^\mu(\omega) = \bar{Q}_v\, \{iD^\mu, \delta(iD_+ + \omega)\}\, Q_v \tag{24}$$
$$O_2^\mu(\omega) = i\bar{Q}_v\, [iD^\mu, \delta(iD_+ + \omega)]\, Q_v$$
$$O_3^{\mu\nu}(\omega_1, \omega_2) = \tag{25}$$
$$\bar{Q}_v \delta(iD_+ + \omega_2)\, \{iD_\perp^\mu, iD_\perp^\nu\}\, \delta(iD_+ + \omega_1) Q_v$$
$$O_4^{\mu\nu}(\omega_1, \omega_2) =$$
$$g_s \bar{Q}_v \delta(iD_+ + \omega_2) G_\perp^{\mu\nu} \delta(iD_+ + \omega_1) Q_v\,,$$

plus the corresponding ones where a Pauli spin matrix appears between the quark spinors.

The effect of the subleading terms can be parametrized by four universal functions, which appear again in both $b \to u\ell\bar{\nu}$ and $b \to s\gamma$. Using a simple but realistic model the effects of the subleading terms may be estimated as a function of the lower photon energy cut. In Fig. 3 we plot the rate integrated from a lower cut as a function of this cut for various values of the parameters. As expected, the subleading terms at cut values of 2.3 GeV are of order 10% and negligibly small below 2.1 GeV.

4 "New Physics" in $b \to s\gamma$

In the Standard Model, $b \to s\gamma$ is a loop-induced process; it thus has considerable sensitivity to new physics effects. However, as already pointed out in the introduction, any B physics experiment tests the coefficients c_i appearing in the effective Hamiltonian (1) and thus all the information on new effects is encoded in combinations of the low-energy parameters c_i, which have to be computed

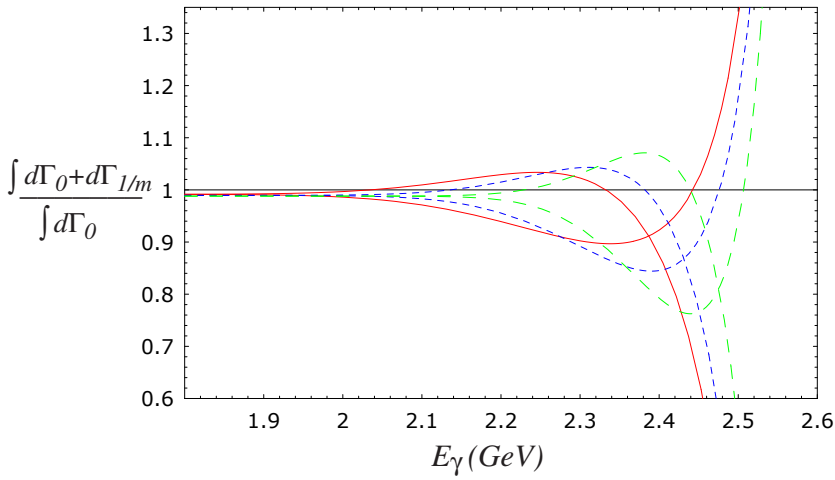

Fig. 3. Partially integrated rate normalized to the leading twist result. The three lines with a peak correspond to $\rho_2 = (500\ \text{MeV})^3$, and $\bar{\Lambda} = 570$ MeV (solid line), $\bar{\Lambda} = 470$ MeV (short-dashed line) $\bar{\Lambda} = 370$ MeV (long-dashed line). The two lines with a dip have $\rho_2 = -(500\ \text{MeV})^3$ and $\bar{\Lambda} = 470$ MeV (dashed line), $\bar{\Lambda} = 370$ MeV (dotted line).

in the Standard Model with the best possible accuracy. Comparing this to B decay data, it will clearly be impossible to find clean evidence for some specific scenario of new physics.

At present, no significant deviation from the Standard Model has been observed in $B \to X_s\gamma$ nor in any other B decay. Given that there are processes that are sensitive to new effects, B physics (and $b \to s\gamma$ in particular) can contribute to constrain new physics scenarios.

Keeping this in mind one may try various scenarios of new physics and calculate the effects on $b \to s\gamma$, i.e. calculate the coefficients of the low energy effective Hamiltonian (1) in specific scenarios. There is an enormous variety of models for physics beyond the Standard Model on the market, and is is impossible to cover all these ideas.

For that reason I shall only consider two examples, which are instructive and demonstrate the kind of sensitivity one may expect. In the next subsection I shall consider the Type-II two-Higgs doublet model and in Sect. 4.2 I shall discuss a few recent papers on supersymmetry with large values of $\tan\beta$.

4.1 Two-Higgs-Doublet Model (Type II)

One popular and consistent way to extend the Standard Model is to add one or more Higgs doublets. This can be done in various ways, but one well motivated way is to have two Higgs doublets where one doublet gives the mass to the up quarks, the other doublet to the down quarks.

Out of the eight degrees of freedom of the Higgs sector, three are needed to give mass to the heavy weak bosons, while the other five become physical states.

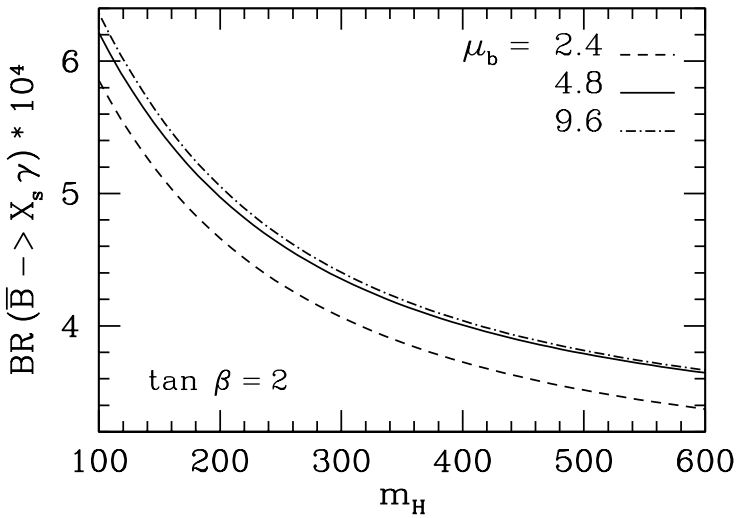

Fig. 4. The branching ratio for $B \to X_s\gamma$ as a function of the charged Higgs mass; figure taken from [29].

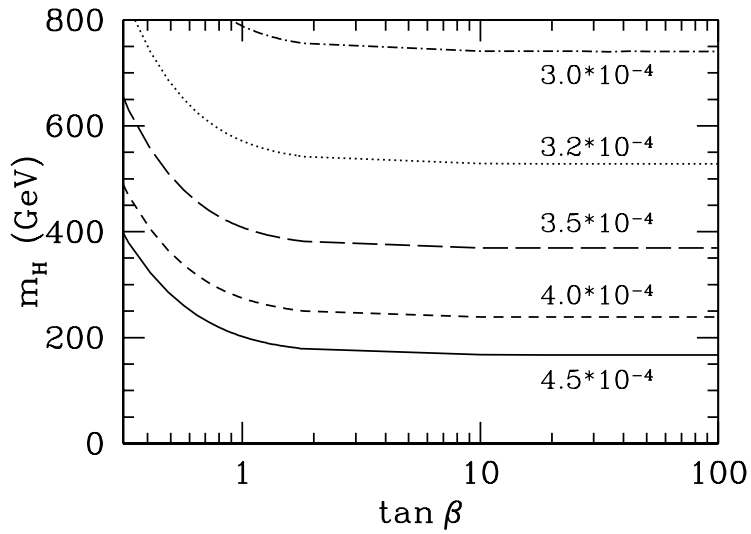

Fig. 5. The $\tan\beta$-M_{H^+} plane; contours indicate different experimental values for $B \to X_s\gamma$; figure taken from [29].

In particular, the spectrum contains a charged Higgs boson, which appears in the loops relevant to $b \to s\gamma$. The first analysis of this decay in this type of two-Higgs doublet model has been performed in [28].

The parameters of this model are the ratio of the two vacuum expectation values (usually expressed as $\tan\beta = v_1/v_2$), the mass M_{H^+} of the charged Higgs boson, all other parameters are irrelevant for our discussion.

In Fig. 4 (taken from [29]) the branching ratio of $b \to s\gamma$ is plotted as a function of the charged Higgs mass, for three different values of the renormalization scale μ.

In Fig. 5 (taken from [29]) we plot contours in the $\tan\beta$–M_{H^+} plane for different values of the $B \to X_s\gamma$ branching ratio. From this figure it becomes clear that there is no large effect induced by enlarging $\tan\beta$. One may derive bounds on the charged Higgs mass independently of $\tan\beta$; the current bound is $M_{H^+} > 314$ GeV at 95% CL [30].

4.2 Supersymmetry with Large $\tan\beta$

If supersymmetry were an exact symmetry, $b \to s\gamma$ would vanish, owing to the cancellations between particles and sparticles [31]. This means that $b \to s\gamma$ tests the breaking of supersymmetry. Clearly many different scenarios for this symmetry breaking can be invented, having complicated flavour structure.

Again I shall pick an example from a recent analysis [32,33]. In these papers it has been pointed out that $B \to X_s\gamma$ can indeed be enhanced in scenarios whith large $\tan\beta$. Working in the MSSM with a flavour-diagonal supersymmetry-breaking sector, the relevant parameters are the charged Higgs mass M_{H^+}, the light stop mass $m_{\tilde{t}_1}$, the supersymmetric μ parameter, and the parameter A_t from the sector of soft-supersymmetry breaking.

For large $\tan\beta$, renormalization group methods may be used to resum these terms [33] and one may confront these results with the recent data. In Fig. 6 (taken from [33]) we plot the rate for $B \to X_s\gamma$ as a function of $\tan\beta$ for $\mu = \pm 500$ GeV; the values of the other parameters are $M_{H^+} = 200$ GeV, $m_{\tilde{t}_1} = 250$ GeV, all other sparticle masses being at 800 GeV.

A similar plot can be made for negative A_t, but for the parameters chosen here this scenario is already practically excluded.

Given such a scenario, one may also scan over some range for the parameters and identify regions that are still allowed by the experimental constraints. In Fig. 7 such a scan was performed with $m_{\tilde{t}_2} \le m_{\tilde{t}_1} \le 1$ TeV, $m_{\tilde{\chi}_2^+} \le m_{\tilde{\chi}_1^+} \le 1$ TeV, $|A_t| \le 500$ GeV, all other sparticle masses being 1 TeV.

Clearly $B \to X_s\gamma$ places significant constraints on the parameter space of certain supersymmetric scenarios; however, these studies have been performed with a flavour diagonal supersymmetry-breaking sector. An analysis witout this constraint can be found in [34]

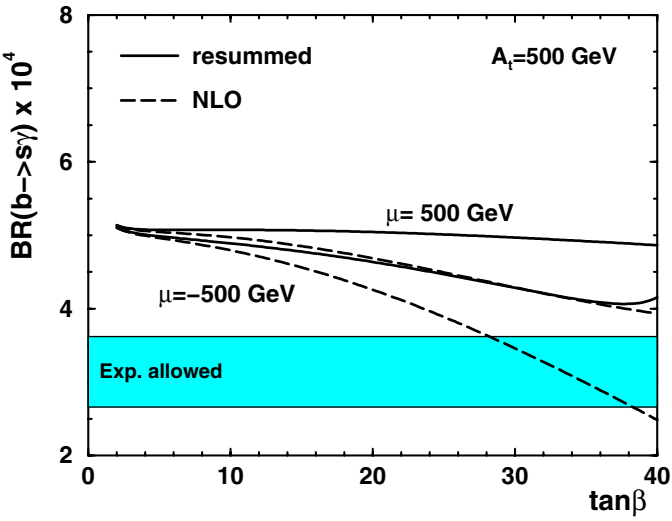

Fig. 6. The rate for $B \to X_s\gamma$ versus $\tan\beta$; for the values of the parameters see text. Figure taken from [33].

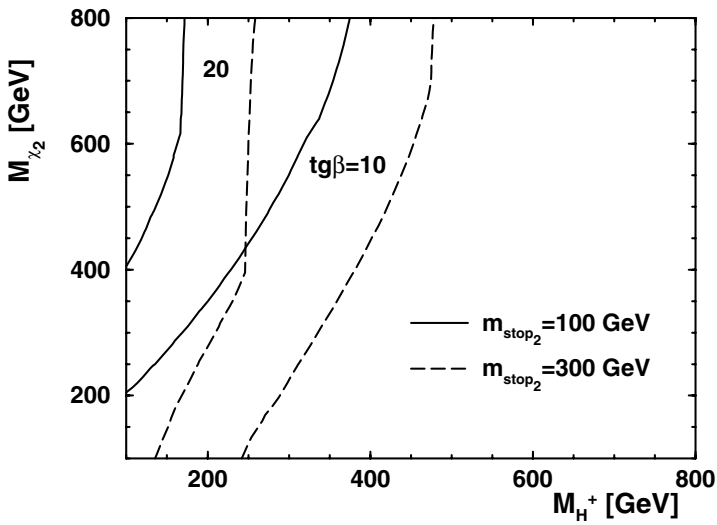

Fig. 7. Allowed range in the M_{H^+}–$M_{\tilde{\chi}2}$ plane for different values of $\tan\beta$ for two values of $m_{\tilde{t}_2}$. Figure taken from [33].

5 Summary on $b \to s\gamma$

The inclusive radiative rare decay $B \to X_s\gamma$ is under reasonable theoretical control; the latest theoretical prediction [18] is slightly higher than (9)

$$Br_{th}(B \to X_s\gamma) = (3.71 \pm 0.30) \times 10^{-4}\,,$$

where the difference originates from a different value for the ratio m_c/m_b; while [16] use the ratio of pole masses, in [18] $m_c^{\overline{MS}}/m_b^{Pole}$ is is used as an "educated guess" of NNLO corrections.

The latest (combined) experimental result is [18]

$$Br_{exp} = (B \to X_s\gamma) = (2.96 \pm 0.35) \times 10^{-4}\,, \tag{26}$$

which is in agreement with theory within 1.6σ.

The theoretical uncertainty is mainly determined by our ignorance of some of the input parameters (quark masses, mixing angles) and to some extent also by the uncertainty of higher-order radiative corrections. Improving the current theoretical uncertainty will be very difficult with current theoretical tools.

6 The Inclusive Decay $B \to X_s\ell^+\ell^-$

6.1 Differential Rate and Forward-Backward Asymmetry

We make again use of the heavy mass expansion in which case the differential rates for the inclusive process $B \to X_s\ell^+\ell^-$ to leading order is given by the partonic rate. The quantities we are going to consider in some detail are the invariant mass spectrum ($\hat{s} = s/m_b^2$) of the leptons and the forward backward asymmetry defined by

$$\mathcal{A}(\hat{s}) \equiv \int_0^1 dz\, \frac{d^2\mathcal{B}}{dz\, d\hat{s}}(B \to X_s\ell^+\ell^-) - \int_{-1}^0 dz\, \frac{d^2\mathcal{B}}{dz\, d\hat{s}}(B \to X_s\ell^+\ell^-). \tag{27}$$

where $d^2\mathcal{B}/(dz\, d\hat{s})$ is the doubly differential rate with $z \equiv \cos\theta$, where θ is the angle of the ℓ^+ with respect to the b-quark direction in the centre-of-mass system of the dilepton pair.

Defining the kinematic variables as

$$\begin{aligned} u &= (p_b - p_1)^2 - (p_b - p_2)^2, \\ s &= (p_1 + p_2)^2, \\ \hat{s} &= \frac{s}{\mathrm{mb}^2}, \\ w(s) &= \sqrt{(s - (\,\mathrm{mb} + m_s)^2)(s - (\,\mathrm{mb} - m_s)^2)}. \end{aligned} \tag{28}$$

where p_b, p_1 and p_2 denote, respectively, the momenta of the b quark ($= B$ hadron), ℓ^+ and ℓ^-, we obtain for the leptonic invariant mass spectrum

$$\frac{d\mathcal{B}}{d\hat{s}} = \mathcal{B}_{sl}\frac{\alpha^2}{4\pi^2}\frac{|V_{tb}V_{ts}^*|^2}{|V_{cb}|^2}\frac{1}{f(m_c^2/m_b^2)}w(\hat{s})\left[\left(|C_9+Y(\hat{s})|^2+C_{10}^2\right)\alpha_1(\hat{s},\hat{m}_s)\right. \quad (29)$$
$$\left.+\frac{4}{\hat{s}}C_7^2\alpha_2(\hat{s},\hat{m}_s)+12\alpha_3(\hat{s},\hat{m}_s)C_7(C_9+\ \mathrm{Re}\ Y(s))\right],$$

where f is the usual phase space function appearing in the calculation of the inclusive semileptonic rate

$$f(x) = 1-8x-8x^3-x^4-12x^2\ln x \quad (30)$$

the auxiliary functions are defined as follows:

$$\alpha_1(\hat{s},\hat{m}_s) = -2\hat{s}^2+\hat{s}(1+\hat{m}_s^2)+(1-\hat{m}_s^2)^2, \quad (31)$$
$$\alpha_2(\hat{s},\hat{m}_s) = -(1+\hat{m}_s^2)\hat{s}^2-(1+14\hat{m}_s^2+\hat{m}_s^4)\hat{s}+2(1+\hat{m}_s^2)(1-\hat{m}_s^2)^2, \quad (32)$$
$$\alpha_3(\hat{s},\hat{m}_s) = (1-\hat{m}_s^2)^2-(1+\hat{m}_s^2)\hat{s}, \quad (33)$$
$$Y(\hat{s}) = g(m_c/m_b,\hat{s})(3C_1+C_2+3C_3+C_4+3C_5+C_6) \quad (34)$$
$$-\frac{1}{2}g(1,\hat{s})(4C_3+4C_4+3C_5+C_6)$$
$$-\frac{1}{2}g(0,\hat{s})(C_3+3C_4)+\Delta C_9,$$

and $g(z,\hat{s})$ is the one-loop function given by

$$\mathrm{Re}\ g(z,s) = -\frac{4}{9}\ln z^2+\frac{8}{27}+\frac{16z^2}{9s} \quad (35)$$
$$-\frac{2}{9}\sqrt{1-\frac{4z^2}{s}}\left(2+\frac{4z^2}{s}\right)\ln\left|\frac{1+\sqrt{1-\frac{4z^2}{s}}}{1-\sqrt{1-\frac{4z^2}{s}}}\right| \quad \text{for } s>4z^2$$

$$\mathrm{Re}\ g(z,s) = -\frac{4}{9}\ln z^2+\frac{8}{27}+\frac{16z^2}{9s} \quad (36)$$
$$-\frac{2}{9}\sqrt{1-\frac{4z^2}{s}}\left(2+\frac{4z^2}{s}\right)\ \mathrm{atan}\left(\frac{1}{\sqrt{\frac{4z^2}{s}-1}}\right) \quad \text{for } s<4z^2$$

$$\mathrm{Im}\ g(z,s) = -\frac{2\pi}{9}\sqrt{1-\frac{4z^2}{s}}\left(2+\frac{4z^2}{s}\right)\Theta(s-4z^2). \quad (37)$$

The constant ΔC_9 is given by

$$\Delta C_9(\mu) = \frac{C_9(\mu)}{\alpha_s(\mu)}-\frac{C_9(M_W)}{\alpha_s(M_W)}, \quad (38)$$

and takes into account the fact that the one-loop matrix elements of the operators $\mathcal{O}_1\cdots\mathcal{O}_6$ contains a large logarithm of the form $\ln(M_W^2/m_b^2)$, which is not due to

QCD effects. The one-loop function $g(z, \hat{s})$ is a finite piece and the choice of the renormalization scheme will effect the value of the one-loop function as well as the corresponding value of C_9. The term ΔC_9 cancels this scheme dependence,

In the same way the differential asymmetry as defined in (27) is [35]

$$\mathcal{A}(\hat{s}) = -\mathcal{B}_{sl}\frac{3\alpha^2}{8\pi^2}\frac{C_{10}}{f(m_c/m_b)}w^2(\hat{s})\left[\hat{s}(C_9 + \text{ Re } Y(\hat{s})) + 4C_7(1+\hat{m}_s^2)\right]. \quad (39)$$

Using these two observables we may perform an analysis of new physics effects by taking the Wilson coefficiencts to be free parameters to be determined from experiment.

6.2 Model Independent Analysis of New Physics Effects in $B \to X_s\ell^+\ell^-$ and $B \to X_s\gamma$

In this section we shall discuss how the Wilson coefficients appearing in the effective Hamiltonian may be extracted from the experimental information. The argumentation follows closely the one in [4] We shall assume that all the matrix elements are normalized at the scale $\mu \sim m_b$, the mass of the b quark and hence the decay distributions are given in terms of the Wilson coefficients at the scale m_b. The SM makes specific predictions for these coefficients, but if there is physics beyond the SM, these coefficients will in general be modified.

We will somewhat elaborate on this point. A specific model provides the set of Wilson coefficients at high scales, which we shall choose to be the scale of the weak bosons $\mu = M_W$. Furthermore, we shall integrate out heavy degrees of freedom at the same scale $\mu = M_W$; this procedure introduces an uncertainty due to the difference in the masses of the heavy degrees of freedom. However, since the QCD coupling constant is small at these very high scales and does not appreciably change between these thresholds, it is a reasonably accurate approximation to neglect QCD corrections for scales above $\mu = M_W$. Starting from this scale, the Wilson coefficients are obtained from the solution of the renormalization group equations at the scale $\mu \sim m_b$, where we use the one-loop result for the anomalous dimensions and the beta function (see appendix).

In order to determine the sign of C_7 and the other two coefficients C_9 and C_{10}, one has to study the decay distributions and rates in $B \to X_s\ell^+\ell^-$, where ℓ is either electron or muon. As already discussed, these decays are sensitive to the sign of C_7, and to C_9 and C_{10}. The first experimental information available in the decay $B \to X_s\ell^+\ell^-$ will be a measurement of the branching fraction in a certain kinematic region of the invariant mass s of the lepton pair. In order to minimize long-distance effects we shall consider the kinematic regime for s below the J/ψ mass (low invariant mass) and for s above the mass of the ψ' (high invariant mass). Integrating (20) over these regions for the invariant mass one finds[2]

$$\mathcal{B}(\Delta s) = A(\Delta s)\left(C_9^2 + C_{10}^2\right) + B(\Delta s)C_9 + C(\Delta s), \quad (40)$$

[2] In performing the integrations over Δs we have set the resolution parameter δ to zero, since we do not consider any long-distance contribution. The long-distance

where A, B and C are fixed in terms of the Wilson coefficients $C_1 \cdots C_6$ and C_7. We derive from (29):

$$A(\Delta s) = \mathcal{B}_{sl}\frac{\alpha^2}{4\pi^2}\frac{1}{f(m_c/m_b)}\int\limits_{\Delta s} d\hat{s}\,\hat{u}(\hat{s})\alpha_1(\hat{s},\hat{m}_s) \tag{41}$$

$$B(\Delta s) = \mathcal{B}_{sl}\frac{\alpha^2}{4\pi^2}\frac{1}{f(m_c/m_b)}\int\limits_{\Delta s} d\hat{s}\,\hat{u}(\hat{s})\left[2\alpha_1(\hat{s},\hat{m}_s)\ \mathrm{Re}\ Y(\hat{s}) + 12C_7\alpha_3(\hat{s},\hat{m}_s)\right] \tag{42}$$

$$C(\Delta s) = \mathcal{B}_{sl}\frac{\alpha^2}{4\pi^2}\frac{1}{f(m_c/m_b)}\int\limits_{\Delta s} d\hat{s}\,\hat{u}(\hat{s})\left[\alpha_1(s,\hat{m}_s)\left\{(\ \mathrm{Re}\ Y(\hat{s}))^2 + (\ \mathrm{Im}\ Y(\hat{s}))^2\right\}\right.$$
$$\left. + \frac{4}{s}|C_7|^2\alpha_2(s,\hat{m}_s) + 12\alpha_3(s,\hat{m}_s)C_7\ \mathrm{Re}\ Y(\hat{s})\right], \tag{43}$$

where the auxiliary functions α_i, $i = 1, 2, 3$, are as given above.

In our analysis we keep the values for $C_1 \cdots C_6$ and the modulus of C_7 fixed and hence $A(\Delta s)$, $B(\Delta s)$ and $C(\Delta s)$ may be calculated for the two invariant-mass ranges of interest. For the numerical analysis we use $m_b = 4.7$ GeV, $m_c = 1.5$ GeV, $m_s = 0.5$ GeV. The resulting coefficients A, B, and C are listed in Table 2.

Table 2. Values for the coefficients $A(\Delta s)$, $B(\Delta s)$ and $C(\Delta s)$ for the decay $B \to X_s\ell^+\ell^-$.

Δs	C_7	$A(\Delta s)/10^{-8}$	$B(\Delta s)/10^{-8}$	$C(\Delta s)/10^{-8}$ $\ell = e$	$C(\Delta s)/10^{-8}$ $\ell = \mu$
$4m_\ell^2 < s < m_{J/\psi}^2$	$+0.3$	2.86	-5.76	84.1	76.6
$4m_\ell^2 < s < m_{J/\psi}^2$	-0.3	2.86	-20.8	124	116
$m_{\psi'}^2 < s < (1 - m_s^2)$	$+0.3$	0.224	-0.715	0.654	0.654
$m_{\psi'}^2 < s < (1 - m_s^2)$	-0.3	0.224	-1.34	2.32	2.32

Inspection of (43) shows that the integrand for $C(\Delta s)$ behaves as $1/s$ for small values of s, leading to a logarithmic dependence of $C(\Delta s)$ on the lepton mass for the case of the low invariant mass region. In fact, this is the only point where the masses of the leptons enter our analysis, and from this one may obtain the corresponding coefficients for $\ell = \mu$:

$$C(4m_\mu^2 < s < m_{J/\psi}^2) = C(4m_e^2 < s < m_{J/\psi}^2) - 8|C_7|^2(1+\hat{m}_s^2)(1-\hat{m}_s^2)^3 \ln\left(\frac{m_\mu^2}{m_e^2}\right). \tag{44}$$

Of course one may apply (44) also to obtain C for any other lower cut s_0 on the lepton invariant mass, as long as $s_0 \ll m_{J/\psi}^2$.

contribution peaks strongly at the J/ψ and ψ' and δ has to be several times the width of these resonances in order to avoid large long-distance effects. However, calculating only the short-distance part one may safely neglect δ, since the short-distance contribution is flat in this region.

For a measured branching fraction $\mathcal{B}(\Delta s)$, one can solve the above equation for $\mathcal{B}(\Delta s)$, obtaining concentric circles in the C_9-C_{10} plane, with their centre lying at $C_9^* = B(\Delta s)/(2A(\Delta s))$ and $C_{10}^* = 0$. The radius R of these circles is proportional to

$$R = \sqrt{\mathcal{B}(\Delta s) - \mathcal{B}_{min}(\Delta s)}, \tag{45}$$

where the minimum branching fraction

$$\mathcal{B}_{min}(\Delta s) = C(\Delta s) - \frac{B^2(\Delta s)}{4A(\Delta s)} \tag{46}$$

is determined mainly by the present data on $B \to X_s\gamma$, i.e. by $|C_7|$. For the cases of interest one obtains, with the help of Table 2:

$$\mathcal{B}_{min}(4m_e^2 < s < m_{J/\psi}^2) = \begin{cases} 8.1 \times 10^{-7} \text{ for } C_7 = 0.3 \\ 8.6 \times 10^{-7} \text{ for } C_7 = -0.3, \end{cases} \tag{47}$$

$$\mathcal{B}_{min}(m_{\psi'}^2 < s < (1 - m_s^2)) = \begin{cases} 8.5 \times 10^{-10} \text{ for } C_7 = 0.3 \\ 3.0 \times 10^{-9} \text{ for } C_7 = -0.3. \end{cases} \tag{48}$$

Note that $\mathcal{B}(\Delta s)$ is an even function of C_{10}, so one is not able to fix the sign of C_{10} from a measurement of $\mathcal{B}(\Delta s)$ alone.

To further pin down the Wilson coefficients, one could perform a measurement of the forward-backward asymmetry $\mathcal{A}$, which has been defined above. The asymmetry is an odd function of C_{10}, and for a fixed value of the total branching ratio in this kinematic region one obtains, from integrating over a range (Δs):

$$\mathcal{A}(\Delta s) = C_{10} \left(\alpha(\Delta s) C_9 + \beta(\Delta s)\right), \tag{49}$$

where

$$\alpha(\Delta s) = -\mathcal{B}_{sl} \frac{3\alpha^2}{8\pi^2} \frac{1}{f(m_c/m_b)} \int_{\Delta s} d\hat{s}\, \hat{u}^2(\hat{s}) \hat{s} \tag{50}$$

$$\beta(\Delta s) = -\mathcal{B}_{sl} \frac{3\alpha^2}{8\pi^2} \frac{1}{f(m_c/m_b)} \int_{\hat{s}} d\hat{s}\, \hat{u}^2(\hat{s}) \left[\hat{s}\ \mathrm{Re}\ Y(\hat{s}) + 4C_7(1 + \hat{m}_s^2)\right]. \tag{51}$$

For a fixed value of $\mathcal{A}(\Delta s)$, one obtains hyperbolic curves in the C_9-C_{10} plane; like the coefficients A, B and C, the parameters α and β are given in terms of the Wilson coefficients $C_1 \cdots C_6$ and C_7, and the kinematic region of s considered; their values are presented in Table 3.

Given the two experimental inputs, the branching fraction $\mathcal{B}(\Delta s)$ and the corresponding asymmetry $\mathcal{A}(\Delta s)$, one obtains a fourth-order equation for the Wilson coefficients C_9 and C_{10}, which admits in general four solutions. In Figs. 8–10 we plot the contours for a fixed value for the branching fraction $\mathcal{B}(\Delta s)$ and the FB asymmetry $\mathcal{A}(\Delta s)$. Since $\mathcal{B}(\Delta s)$ is an even function of C_{10} and $\mathcal{A}(\Delta s)$ is an odd one, we only plot positive values for C_{10}. The asymmetry vanishes

Table 3. Values for the coefficients $\alpha(\Delta s)$and $\beta(\Delta s)$.

Δs	C_7	$\alpha(\Delta s)/10^{-9}$	$\beta(\Delta s)/10^{-9}$
$4m_\ell^2 < s < m_{J/\psi}^2$	$+0.3$	-6.08	-24.0
$4m_\ell^2 < s < m_{J/\psi}^2$	-0.3	-6.08	55.4
$m_{\psi'}^2 < s < (1-m_s^2)$	$+0.3$	-0.391	0.276
$m_{\psi'}^2 < s < (1-m_s^2)$	-0.3	-0.391	1.37

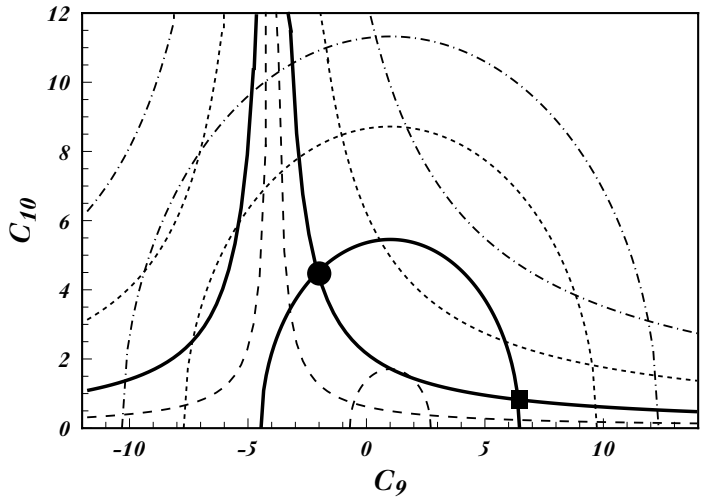

Fig. 8. Contour plots of $\mathcal{B}(\Delta s)$ and $\mathcal{A}(\Delta s)$ in the C_9-C_{10} plane for the low-invariant-mass region $4m_\ell^2 < s < m_{J/\psi}^2$ and $C_7 = 0.3$. The circles correspond to fixed values of $\mathcal{B}$: $\mathcal{B} = 5.6\times10^{-6}$ (solid curve), $\mathcal{B} = 3.0\times10^{-6}$ (long-dashed curve), $\mathcal{B} = 1.0\times10^{-5}$ (short-dashed curve), $\mathcal{B} = 1.5\times10^{-5}$ (dash-dotted curve). The left branches of the hyperbolae correspond to positive values of $\mathcal{A}$: $\mathcal{A} = 1.7\times10^{-7}$ (solid curve), $\mathcal{A} = 5.0\times10^{-8}$ (long-dashed curve), $\mathcal{A} = 5.0\times10^{-7}$ (short-dashed curve), $\mathcal{A} = 1.0\times10^{-6}$ (dash-dotted curve). The right branches of the hyperbolae correspond to negative values of $\mathcal{A}$: $\mathcal{A} = -1.41\cdot10^{-8}$ (solid curve), $\mathcal{A} = -5.0\cdot10^{-9}$ (long-dashed curve), $\mathcal{A} = -3.0\cdot10^{-8}$ (short-dashed curve), $\mathcal{A} = -6.0\cdot10^{-8}$ (dash-dotted curve). For negative values of C_{10}, the figure is simply reflected with $\mathcal{A} \to -\mathcal{A}$. The solid dot indicates the SM values for C_9 and C_{10}. The solid square is another allowed solution resulting from the SM values of $\mathcal{B}$ and $\mathcal{A}$.

for $C_{10} = 0$, but also for $C_9 = -\beta(\Delta s)/\alpha(\Delta s)$. The two lines $C_{10} = 0$ and $C_9 = -\beta(\Delta s)/\alpha(\Delta s)$ divide the C_9-C_{10} plane into four quadrants, in which the asymmetry has a definite sign. Reflecting the hyperbolae on the line $C_{10} = 0$ or $C_9 = -\beta(\Delta s)/\alpha(\Delta s)$ results in a sign change of the asymmetry.

Figures 8 and 9 show the contours in the $C_9(\mu)$-$C_{10}(\mu)$ plane for the low-invariant-mass region $4m_e^2 < s < m_{J/\psi}^2$, and Fig. 10 is for the high-invariant-mass region $m_{\psi'}^2 < s < (1-\hat{m}_s)^2$. Figures 8 and 10 are obtained for $C_7(\mu) = 0.3$, while Fig. 9 is for $C_7(\mu) = -0.3$. The possible solutions for C_9 and C_{10} are given by the intersections of the circle corresponding to the measured branching fraction

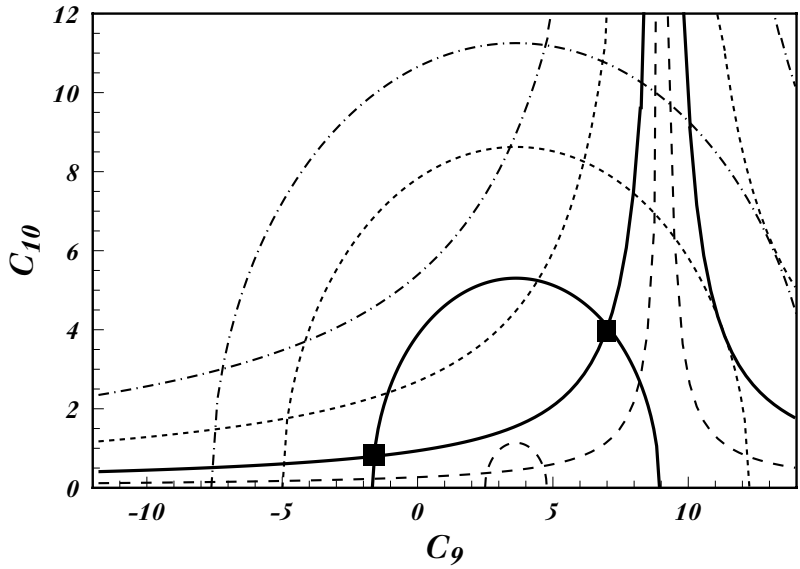

Fig. 9. Same as in Fig. 1, but for $C_7 = -0.3$.

and the hyperbola, corresponding to the measured asymmetry. Assuming the SM values for both $\mathcal{B}(\Delta s)$ and $\mathcal{A}(\Delta s)$, one obtains the solid lines in Figs. 8–10. The possible solutions in this case are represented by solid dots (SM solutions) and solid squares (other non-SM possible solutions).

From the figures one reads off that for the SM values of $\mathcal{B}$ and $\mathcal{A}$ one has more than one solution for the coefficients C_9 and C_{10}, but the ambiguity may in general be resolved by measuring both the low and the high invariant mass regions.

However, there is in principle also the possibility that the equations do not have a solution for C_9 and C_{10}. This is the case, for example, when the asymmetry is large and the branching fraction small, in which case the hyperbola may not intersect with the corresponding circle any more. If this happens one has to conclude that the present analysis is not complete; in other words, the operator basis we started from is not complete and physics beyond the SM will be present in the form of additional operators such as right-handed currents.

7 Conclusions

Rare decays mediated through flavour changing neutral current processes provide an important testing ground of the flavour structure of the standard model. In particular, the inclusive decays of B mesons – due to the large mass of the b quark – can be treated from the theoretical side in a systematic way. The main tool at our disposal is the expansion in inverse powers of the heavy quark mass, which allows us to make clean theoretical predictions including estimates of uncertainties. Such an estimate is indispensable to pin down any effect of physics

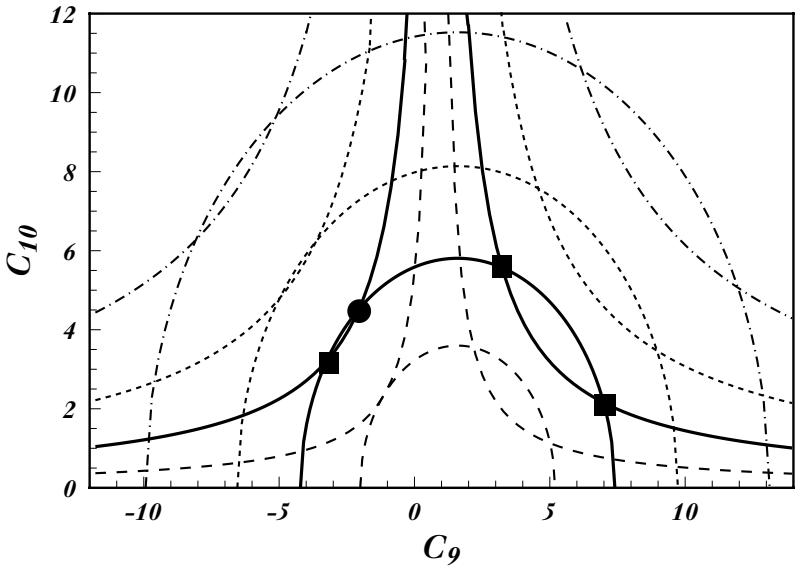

Fig. 10. Contour plots of $\mathcal{B}(\Delta s)$ and $\mathcal{A}(\Delta s)$ in the C_9-C_{10} plane for the high-invariant-mass region $m^2_{\psi'} < s < (1 - m_s)^2$ and for $C_7 = 0.3$. The circles correspond to fixed values of $\mathcal{B}$: $\mathcal{B} = 2.56 \times 10^{-7}$ (solid curve), $\mathcal{B} = 1.0 \times 10^{-7}$ (long-dashed curve), $\mathcal{B} = 5.0 \times 10^{-7}$ (short-dashed curve), $\mathcal{B} = 1.0 \times 10^{-6}$ (dash-dotted curve). The left branches of the hyperbolae correspond to positive values of $\mathcal{A}$: $\mathcal{A} = 1.41 \times 10^{-8}$ (solid curve), $\mathcal{A} = 5.0 \times 10^{-9}$ (long-dashed curve), $\mathcal{A} = 3.0 \times 10^{-8}$ (short-dashed curve), $\mathcal{A} = 6.0 \times 10^{-8}$ (dash-dotted curve). The right branches of the hyperbolae correspond to negative values of $\mathcal{A}$: $\mathcal{A} = -1.41 \times 10^{-8}$ (solid curve), $\mathcal{A} = -5.0 \times 10^{-9}$ (long-dashed curve), $\mathcal{A} = -3.0 \times 10^{-8}$ (short-dashed curve), $\mathcal{A} = -6.0 \times 10^{-8}$ (dash-dotted curve). For negative values of C_{10}, the figure is simply reflected with $\mathcal{A} \to -\mathcal{A}$. The solid dot indicates the SM Values for C_9 and C_{10}. The solid squares are other allowed solutions resulting from the SM values of $\mathcal{B}$ and $\mathcal{A}$.

beyond the Standard model in a unique way. In the meantime, many perturbative and nonperturbative contributions to rare decays have been identified and calculated in the standard model, and in particular the inclusive rare decays are under reasonable theoretical control.

Many scenarios of new physics have been invented. However, in B meson decays we can only obtain a limited ammount of information, which cannot finally settle the question of the details of physics beyond the standard model. The information that can be extracted is encoded in the Wilson coefficients of the effective Hamiltonian mediating the decays under study. In turn, this may as well be used as a model independent way to analyse B decays. Focussing on the Wilson coefficients which correspond to loop processes (i.e. $C_7, C_9 and C_{10}$), one may calculate certain observables as a function of these coeffients and – by measuring the values of these coefficients – try to extract the value of the coefficients.

In the near future the B factories as well as the hadron colliders will produce a large amount of data, including information on FCNC rare decays. Although at present there is no hint to physics beyond the standard model, there is still ample of room for a discovery of first hints at "new physics" at the B factories.

References

1. M. S. Alam *et al.* [CLEO Collaboration], Phys. Rev. Lett. **74**, 2885 (1995).
2. K. Hagiwara *et al.* [Particle Data Group Collaboration], *Review of particle Properties* Phys. Rev. D **66**, 010001 (2002).
3. T. E. Coan *et al.* [CLEO Collaboration], hep-ex/0010075.
4. A. Ali, G. F. Giudice and T. Mannel, Z. Phys. C **67**, 417 (1995) [hep-ph/9408213].
5. A. V. Manohar and M. B. Wise, *Cambridge Monographs on Particle Physics, Nuclear Physics, and Cosmology, Vol. 10.*
6. N. Isgur and M. B. Wise, CEBAF-TH-92-10, appeared in: Stone, S. (ed.): *B physics*, World Scientific 1994, p. 158-209.
7. M. Neubert, Phys. Rept. **245**, 259 (1994) [hep-ph/9306320].
8. I. Bigi, M. Shifman and N. Uraltsev, Ann. Rev. Nucl. Part. Sci. **47**, 591 (1997) [hep-ph/9703290].
9. T. Mannel, Rept. Prog. Phys. **60**, 1113 (1997).
10. G. Buchalla, A. J. Buras and M. E. Lautenbacher, Rev. Mod. Phys. **68**, 1125 (1996) [arXiv:hep-ph/9512380].
11. K. Chetyrkin, M. Misiak and M. Munz, Phys. Lett. B **400**, 206 (1997) [hep-ph/9612313].
12. A. Ali and C. Greub, Z. Phys. C **49**, 431 (1991).
13. K. Adel and Y. Yao, Phys. Rev. D **49**, 4945 (1994) [hep-ph/9308349].
14. C. Greub, T. Hurth and D. Wyler, hys. Lett. B **380**, 385 (1996) [hep-ph/9602281], Phys. Rev. D **54**, 3350 (1996) [hep-ph/9603404].
15. A. Czarnecki and W. J. Marciano, Phys. Rev. Lett. **81**, 277 (1998) [hep-ph/9804252].
16. A. L. Kagan and M. Neubert, Eur. Phys. J. C **7**, 5 (1999) [hep-ph/9805303].
17. A. J. Buras, M. Misiak, M. Munz and S. Pokorski, Nucl. Phys. B **424**, 374 (1994) [hep-ph/9311345].
18. M. Misiak, talk given at the "XXVIII Rencontres de Moriond", 10 - 17 March 2001, Les Arcs, France.
19. M. B. Voloshin, Phys. Lett. B **397**, 275 (1997) [hep-ph/9612483], A. K. Grant, A. G. Morgan, S. Nussinov and R. D. Peccei, Phys. Rev. D **56**, 3151 (1997) [hep-ph/9702380].
20. G. Buchalla, G. Isidori and S. J. Rey, Nucl. Phys. B **511**, 594 (1998) [hep-ph/9705253].
21. Z. Ligeti, L. Randall and M. B. Wise, Phys. Lett. B **402**, 178 (1997) [hep-ph/9702322].
22. M. Neubert, Phys. Rev. D **49**, 4623 (1994) [hep-ph/9312311].
23. I. I. Bigi, M. A. Shifman, N. G. Uraltsev and A. I. Vainshtein, Int. J. Mod. Phys. A **9**, 2467 (1994) [hep-ph/9312359].
24. A. K. Leibovich, I. Low and I. Z. Rothstein, Phys. Lett. B **486**, 86 (2000) [hep-ph/0005124].
25. T. Mannel and S. Recksiegel, Phys. Rev. D **60**, 114040 (1999) [hep-ph/9904475].
26. F. De Fazio and M. Neubert, JHEP**9906**, 017 (1999) [hep-ph/9905351].

27. C. W. Bauer, M. Luke and T. Mannel, hep-ph/0102089.
28. M. Ciuchini, G. Degrassi, P. Gambino and G. F. Giudice, two-Higgs doublet model," Nucl. Phys. B **527** (1998) 21 [hep-ph/9710335].
29. F. M. Borzumati and C. Greub, Phys. Rev. D **58**, 074004 (1998) [hep-ph/9802391].
30. P. Gambino, as in [18]
31. S. Ferrara and E. Remiddi, Phys. Lett. B **53**, 347 (1974).
32. G. Degrassi, P. Gambino and G. F. Giudice, JHEP**0012**, 009 (2000) [hep-ph/0009337].
33. M. Carena, D. Garcia, U. Nierste and C. E. Wagner, Phys. Lett. B **499**, 141 (2001) [hep-ph/0010003].
34. F. Gabbiani, E. Gabrielli, A. Masiero and L. Silvestrini, Nucl. Phys. B **477**, 321 (1996) [hep-ph/9604387], F. Borzumati, C. Greub, T. Hurth and D. Wyler, Phys. Rev. D **62**, 075005 (2000) [hep-ph/9911245].
35. A. Ali, T. Mannel and T. Morozumi, Phys. Lett. B **273**, 505 (1991).